PNAS Nexus, 2023, 2, 1–12
https://doi.org/10.1093/pnasnexus/pgad350
Advance access publication 25 October 2023
Research Report

Interferon ε restricts Zika virus infection in the female reproductive tract

Chuan Xu[a], Annie Wang[a], Laith Ebraham[a], Liam Sullivan[a], Carley Tasker[a], Vanessa Pizutelli[a], Jennifer Couret[b], Cyril Hernandez[a], Priyanka Kolli[c], Pratik Q. Deb[d], Luke Fritzky[d], Selvakumar Subbian[a], Nan Gao[e], Yungtai Lo[f], Mirella Salvatore[g], Amariliz Rivera[b], Alexander Lemenze[d], Patricia Fitzgerald-Bocarsly[d], Sanjay Tyagi[a], Wuyuan Lu[h], Aimee Beaulieu[b,1] and Theresa L. Chang[a,b,*,1]

[a]Public Health Research Institute, Rutgers, New Jersey Medical School, Newark, NJ 07103, USA
[b]Department of Microbiology, Biochemistry and Molecular Genetics, Rutgers, New Jersey Medical School, Newark, NJ 07103, USA
[c]Graduate School of Biological Sciences, Rutgers, New Jersey Medical School, Newark, NJ 07103, USA
[d]Department of Pathology and Laboratory Medicine, Rutgers, New Jersey Medical School, Newark, NJ 07103, USA
[e]Department of Cell Biology, Rutgers, School of Art and Science-Newark, Newark, NJ 07103, USA
[f]Department of Epidemiology and Population Health, Albert Einstein College of Medicine, Bronx, NY 10461, USA
[g]Departmentof Medicine, Weill Cornell Medical College, New York, NY 10065, USA
[h]Key Laboratory of Medical Molecular Virology (MOE/NHC/CAMS), School of Basic Medical Science, and Shanghai Institute of Infectious Disease and Biosecurity, School of Public Health, Fudan University, Shanghai 200032, China
*To whom correspondence should be addressed: Email: theresa.chang@rutgers.edu
[1]A.B. and T.L.C. contributed equally to this work.
Edited By: Victor Nizet

Abstract

Interferon ε (IFNε) is a unique type I IFN that has been implicated in host defense against sexually transmitted infections. Zika virus (ZIKV), an emerging pathogen, can infect the female reproductive tract (FRT) and cause devastating diseases, particularly in pregnant women. How IFNε contributes to protection against ZIKV infection in vivo is unknown. In this study, we show that IFNε plays a critical role in host protection against vaginal ZIKV infection in mice. We found that IFNε was expressed not only by epithelial cells in the FRT but also by immune and stromal cells at baseline or after exposure to viruses or specific Toll-like receptor (TLR) agonists. IFNε-deficient mice exhibited abnormalities in the epithelial border and underlying tissue in the cervicovaginal tract, and these defects were associated with increased susceptibility to vaginal but not subcutaneous ZIKV infection. IFNε deficiency resulted in an increase in magnitude, duration, and depth of ZIKV infection in the FRT. Critically, intravaginal administration of recombinant IFNε protected *Ifnε*$^{-/-}$ mice and highly susceptible *Ifnar1*$^{-/-}$ mice against vaginal ZIKV infection, indicating that IFNε was sufficient to provide protection even in the absence of signals from other type I IFNs and in an IFNAR1-independent manner. Our findings reveal a potentially critical role for IFNε in mediating protection against the transmission of ZIKV in the context of sexual contact.

Significance Statement

Interferon ε (IFNε), a unique type I IFN that is highly expressed in the epithelium of the female reproductive tract (FRT), is thought to protect the host against sexually transmitted infections (STIs), but the mechanism of action is not defined. Zika virus (ZIKV), a causative agent for preterm birth and other severe diseases in pregnant women, can be spread through vaginal transmission. In this study, we show that mice lacking the *Ifnε* gene have abnormal epithelial development and tissue architecture in the cervicovaginal tract. The role of IFNε in protecting the host against ZIKV is FRT-specific and is independent of IFNAR1 signaling. Our findings suggest potential preventive strategies based on harnessing mucosal immunity against STIs.

Introduction

Host defense against microbial invasion in the female reproductive tract (FRT) depends on the maintenance of an effective epithelial barrier and continual surveillance by immune cells in the mucosa. Disruption of barrier function or immune responses in the FRT is associated with sexually transmitted infections (STIs) and other genitourinary infections (1–6). Zika virus (ZIKV) is an emerging flavivirus that is principally transmitted by Aedes mosquitoes but can also be spread through vaginal transmission as an STI (7–11). ZIKV infection can cause severe adverse effects during pregnancy, ranging from preterm birth and miscarriage to microcephaly and other congenital defects in the fetus (12). ZIKV infection has also been associated with diverse pathologies in adults and children, including Guillain–Barré syndrome, myelitis, and neuropathy (13, 14). The cellular and molecular signals that mediate protection against ZIKV infection, particularly in

Competing Interest: The authors declare no competing interest.
Received: April 4, 2023. **Accepted:** October 13, 2023

the context of transmission through sexual contact, remain incompletely understood.

Prior studies in humans and mice have demonstrated an important role for type I interferon (IFN) epsilon, IFNε, in protection against STIs, including HIV, herpes simplex virus 2 (HSV2), ZIKV, and chlamydial infection (15–21), but the mechanism of antiviral activities in vivo was not defined. Although IFNε is classified as a type I IFN, it differs from other type I IFNs, i.e. IFNα and IFNβ, in many respects, including its low (~30%) amino acid homology and distinct expression patterns (15). Indeed, IFNε is constitutively expressed in epithelial cells lining many mucosal tissues including the FRT, whereas IFNα/β expression in these tissues is typically limited to settings of infection or inflammation (22). The mechanisms by which IFNε and other type I IFNs mediate antiviral defense also differ. We have previously shown that IFNε protects human primary macrophages against HIV infection via mechanisms distinct from those of IFNα2, through the induction of reactive oxygen species, distinct proinflammatory cytokines and chemokines, and phagocytosis (21). Moreover, IFNε (at mid ng/mL ranges) has no or only weak antiviral activities in transformed cell lines, while IFNα/β exhibit potent antiviral activities in diverse primary and transformed cell types (21, 23–25).

In this study, we demonstrate a critical role for IFNε in host defense against vaginal ZIKV infection in mice. We find that IFNε-deficient mice are specifically susceptible to ZIKV when challenged via the intravaginal, but not the subcutaneous, route, suggesting that IFNε plays a specific role in protecting against ZIKV transmission in the context of sexual contact. Our data indicate that IFNε is required to maintain normal epithelial and submucosal architecture in the cervicovaginal tissue (CVT) of mice at a steady state, suggesting that IFNε may promote resistance to ZIKV infection by maintaining tissue integrity. Notably, recombinant IFNε is sufficient to protect highly susceptible *Ifnar1*$^{-/-}$ mice from intravaginal ZIKV challenge, suggesting that IFNε provides host protection even in the absence of signals from other type I IFNs, and it mediates this protection through IFNAR1-independent mechanisms. Taken together, our data highlight a novel role for IFNε in maintaining epithelial and tissue structure in the FRT and for mediating FRT-specific protection against ZIKV infection.

Results

IFNε is expressed by epithelial and nonepithelial cells in the FRT

To better understand the steady-state expression patterns of IFNε in vivo, we first assessed *Ifnε* transcript abundance in different organs and mucosal tissues from naïve wild-type (WT) mice. In agreement with a previous study (16), *Ifnε* expression was highest in FRT tissues compared with that in other tissues, although abundant *Ifnε* transcripts were also detected in the lung and intestinal mucosal tissues (Figure 1A). Within the FRT compartment, we found that *Ifnε* expression was highest in the CVT, as compared to the uterus and ovaries. Consistent with our gene expression data, IFNε proteins were readily detected in the epithelium of vaginal and uterine tissues from WT mice (Figure 1B).

To identify specific cell types that express *Ifnε* transcripts in the FRT, we performed RT-qPCR on sort-purified CD45^{+} immune cells, EpCAM^{+} epithelial cells, and CD45^{-}EpCAM^{-} cells from the ovaries, CVT, and uteri of WT mice. *Ifnε* transcripts were most abundant in epithelial cells, but were also detected in immune and nonimmune CD45^{-}EpCAM^{-} cells from the FRT (Figure 1C). IFNε expression in CD45^{-}EpCAM^{-} cells from the CVT raised the possibility of the involvement of stromal cells. Indeed, we detected IFNε proteins in desmin-expressing stromal cells in addition to epithelial cells (Figure S1). These findings suggest that IFNε is expressed by diverse cell types in the FRT, including epithelial cells, stromal cells, and immune cells.

Given our findings of IFNε expression by different cell types in mouse FRT tissue, we assessed IFNε expression in primary human cervical tissue and human peripheral blood mononuclear cells (PBMCs). Consistent with our findings in mice, IFNε protein was readily detectable in the luminal and glandular epithelial cells and in nonepithelial cells distributed throughout the submucosa in cervical tissue from healthy donors (Figure 1D). We also detected *IFNε* transcripts in PBMCs from healthy donors (Figure 1E), although they were less abundant compared with cervical cancer HeLa cells, known to express IFNε (26). These data suggest that immune cells may also serve as a key source of IFNε in humans.

IFNε is induced in response to TLR activation and viral infection

Prior studies reported that mouse bone marrow–derived macrophages (BMDMs) do not express IFNε at baseline or in response to TLR activation or viral infection (16). However, whether inflammatory or infectious stimuli are sufficient to induce IFNε expression in other cell types remains an open question. To address this, we first investigated the impact of stimulation with TLR agonists on IFNε expression in freshly isolated human PBMCs. *IFNε* transcripts were low at baseline but were significantly up-regulated in response to TLR3 or TLR4 activation (Figure 2A). Since activated plasmacytoid dendritic cells (pDCs) produce high levels of IFNα, we also measured IFNε expression in human pDCs exposed to various viruses or cytokines for 4 h. *IFNε* transcripts were undetectable in pDCs at baseline, but were significantly up-regulated in response to the Sendai virus and HSV1 (Figure 2B). IFNε induction was less pronuced by Influenza virus. In contrast, exposure to HIV did not induce detectable IFNε expression in pDCs. Cytokines were less effective than viruses at inducing IFNε expression in pDCs. IFNα induced very low levels of *IFNε* mRNAs in pDCs from some but not all donors, whereas IFN-λ, interleukin 3 (IL-3), and IL-10 did not induce detectable IFNε expression in pDCs from any donor (Figure 2B).

Our studies (Figure 1) identified epithelial cells as key IFNε-expressing cell types in human and mouse FRT tissues at a steady state. To determine whether viral infection further increased IFNε expression in epithelial cells, we measured *IFNε* transcript abundance in primary human cervical epithelial cells (CECs) that were mock-infected or infected with ZIKV for 24 h. Primary CECs expressed low but detectable levels of *IFNε* mRNA at baseline (Figure 2C), which was consistent with our findings of IFNε protein expression by epithelial cells in cervical tissue (Figure 1D). Nevertheless, infection with ZIKV elicited a marked increase in *IFNε* expression in CECs within 24 h postinfection (p.i.; Figure 2C).

To determine whether IFNε expression in the FRT was increased by ZIKV infection in vivo, we challenged WT mice with ZIKV intravaginally and measured *Ifnε* transcript abundance in the CVT on days 1 and 2 p.i. There was a robust increase in IFNε expression in the CVT in response to ZIKV infection (Figure 2D). IFNε proteins were detected in both epithelial and stromal cells in the CVT of ZIKV-infected mice at day 2 p.i. (Figure S2). Taken together, our data indicate that ZIKV and certain other viruses are strong inducers of IFNε expression in diverse cell and tissue types, including human PBMCs, pDCs, and CECs, and mouse CVT.

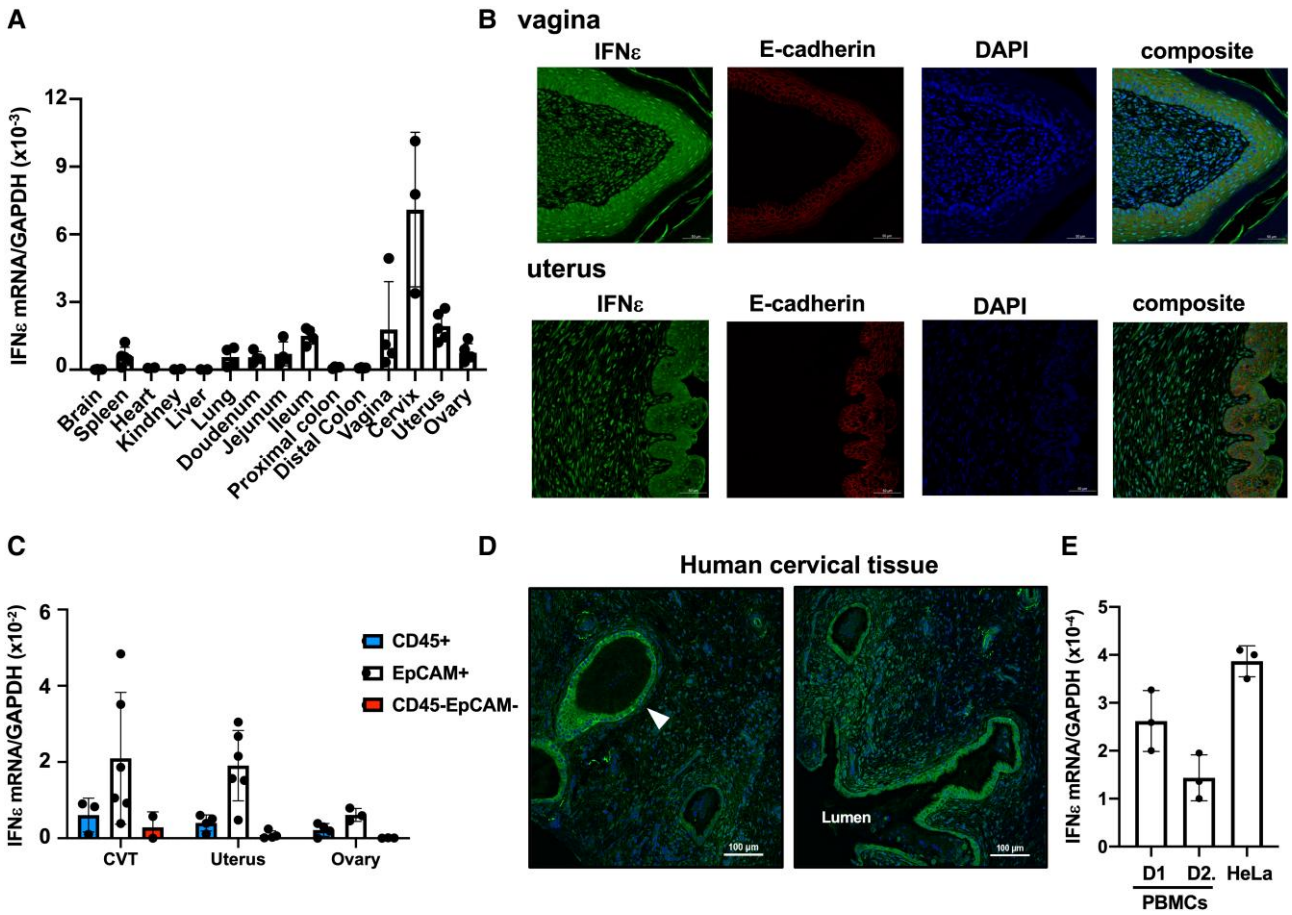

Fig. 1. IFNε is expressed in epithelial and nonepithelial cells in the FRT. A) Total RNAs were extracted from different tissues of WT mice. IFNε mRNA levels were quantified by RT-qPCR and normalized by glyceraldehyde-3-phosphate dehydrogenase (GAPDH) using the $2^{-\Delta\Delta Ct}$ method. Each point represents one animal. B) Expression of IFNε protein in epithelial cells (E-cadherin) in vaginal and uterus tissues. Nuclei were stained with DAPI. C) IFNε mRNA levels were quantified by RT-qPCR of total RNA from sorted immune cells ($CD45^+$), epithelial cells ($EpCAM^+$), and $CD45^-EpCAM^-$ cells from the CVT, uterus, and ovary. D) Detection of human IFNε proteins in human cervical tissues by immunofluorescence staining. The arrow indicates glandular epithelial cells expressing IFNε proteins. E) Total RNAs were extracted from freshly isolated PBMCs from two different donors (D1 and D2). Cervical cancer HeLa cells were included as a positive control. IFNε mRNA levels were quantified by RT-qPCR.

IFNε-deficient mice exhibit abnormal epithelial borders and collagen deposition in the FRT

As a tool to investigate the role of IFNε in protective host responses in vivo, we generated *Ifnε*$^{-/-}$ mice using CRISPR/Cas9 technology (diagrammed in Figure S3). Successful disruption of the *Ifnε* gene was confirmed by genomic sequencing, by loss of *Ifnε* transcripts (Figure 3A), and by loss of protein expression (Figure 3B). We used these mice to investigate the impact of IFNε deficiency on global gene expression in the CVT to identify tissue-level processes regulated by IFNε signaling. Notably, genes identified as differentially expressed in the CVT from naïve *Ifnε*$^{-/-}$ versus WT mice were significantly associated with pathways involved in tissue remodeling and/or epithelial barrier function, including tight junction signaling, fibrosis, epithelial adherens junction signaling, integrin signaling, and actin cytoskeleton signaling pathways (Figure 3C). Moreover, numerous genes encoding collagens, Wnt proteins, tight junction proteins, and chemokines or chemokine receptors were dysregulated in IFNε-deficient tissue (Figure 3D and Table S1).

Wnt signaling critically regulates epithelial homeostasis and impacts the expression and function of collagens involved in tissue integrity and structure (27–32). Our finding of dysregulated expression of both collagen genes and Wnt signaling genes in the CVT from *Ifnε*$^{-/-}$ mice raised the possibility that IFNε signaling may play a role in supporting proper tissue structure in the CVT. We, therefore, analyzed tissue architecture in the CVT of naive *Ifnε*$^{-/-}$ and WT mice (Figure 3E and F). These studies revealed discernible abnormalities in the vaginal fornix (VF) of *Ifnε*$^{-/-}$ mice compared to WT mice, including an underdeveloped epithelial border at the center of the VF and disordered collagen deposition around the vaginal epithelial folds (10×; Figure 3F and G). In addition, epithelial folds located in the central region of the VF were significantly shorter in *Ifnε*$^{-/-}$ mice than in WT mice (Figure 3F–H). *$P<0.05$, WT vs *Ifnε*$^{-/-}$ mice. These findings suggest that IFNε plays an important role in the maintenance of optimal tissue architecture in the CVT, even in the absence of infection.

IFNε is required for resistance to ZIKV infection following vaginal but not subcutaneous challenge

Our findings of abnormal barrier and tissue architecture in the CVT of *Ifnε*$^{-/-}$ mice led us to hypothesize that IFNε may specifically contribute to protection against pathogen entry in the CVT, a common transmission route for STIs. To test this, we challenged hormonally synchronized *Ifnε*$^{-/-}$, WT, and *Ifnar1*$^{-/-}$ mice with ZIKV PRVABC-59 via intravaginal or subcutaneous routes. Hormonal synchronization into diestrus was achieved by administering a subcutaneous

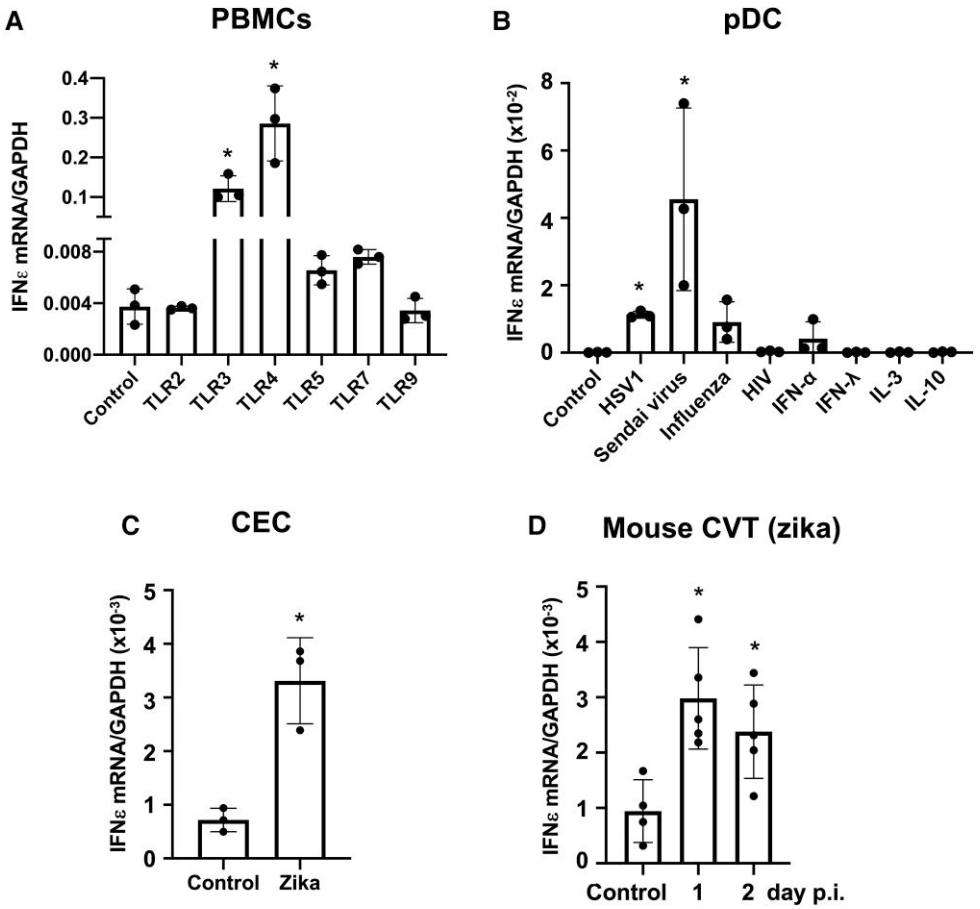

Fig. 2. IFNε is induced in response to viral infection and TLR activation. A) Freshly isolated PBMCs from different donors were stimulated with agonists for TLR2 (Pam3CSK4, 100 ng/mL), TLR3 (poly (I:C), 1 μg/mL), TLR4 (lipopolysaccharide (LPS), 10 ng/mL), TLR5 (FLA-ST, 50 ng/mL), TLR7 (Imiquimod, 500 ng/mL), or TLR9 (ODN2006, 5 μM) for 6 h. Total RNAs were prepared, and IFNε gene expression was quantified by RT-qPCR. B) pDCs from different donors were purified using a negative selection pDC isolation kit. The purified pDCs were untreated (control) or treated with HSV1 2931, Sendai VR 907, influenza virus PR/8/34, HIV-MN, rIFNα, IFNλ, IL-3, or IL-10 for 4 h. Total RNAs were prepared, and IFNε mRNA levels were quantified by RT-qPCR. C) IFNε was determined by RT-qPCR in primary CECs 24 h after ZIKV infection. D) Induction of IFNε gene expression in the cervicovaginal tract of WT mice in response to ZIKV infection. *$P < 0.05$, treated versus untreated controls.

injection of Depo-Provera (Depo). In agreement with published data (9, 33–35), WT mice were more resistant to ZIKV infection than *Ifnar1*$^{-/-}$ mice regardless of the route of infection (Figure 4A). In contrast, *Ifnε*$^{-/-}$ mice were more susceptible to ZIKV infection than WT mice only when challenged via the vaginal route but not when challenged via the subcutaneous route (Figure 4A), supporting our hypothesis that IFNε provides specific protection against vaginal ZIKV transmission. Notably, increased viral loads in vaginally infected *Ifnε*$^{-/-}$ mice were observed only in the CVT, whereas ZIKV RNAs were undetectable in the uteri and spleen of both *Ifnε*$^{-/-}$ and WT mice (Figure 4B). This finding contrasted with the high viral loads in all analyzed tissues from infected *Ifnar1*$^{-/-}$ mice (Figure S4). Viral RNAs were not detected in male *Ifnε*$^{-/-}$ mice or in non-Depo-treated female mice with subcutaneous ZIKV infection (Figure S5), indicating that the absence of detectable virus in subcutaneously challenged *Ifnε*$^{-/-}$ mice was not an artifact of Depo treatment. Collectively, these findings highlight a specific role for IFNε in mediating protection against ZIKV when infection occurs via the vaginal route.

To understand how IFNε signaling impacts the kinetics of ZIKV infection, we assessed viral loads in the CVT of vaginally challenged WT and *Ifnε*$^{-/-}$ mice at different time points after infection. In WT mice, ZIKV RNAs were detectable in the CVT on days 1 and 2 p.i. but undetectable after day 3 p.i. (Figure 4C). In contrast, ZIKV RNA abundance was not only higher in the CVT of *Ifnε*$^{-/-}$ mice as early as day 1 p.i. but also remained detectable until day 8 p.i. (Figure 4C).

We next used single molecule fluorescence in situ hybridization (smFISH) to define the spatial parameters of ZIKV infection within the context of the architecture of the CVT on day 2 p.i. via the vaginal route. Although ZIKV RNA was readily evident in the mid-cervix in both WT and *Ifnε*$^{-/-}$ mice, it was detected only in the proximal cervix in *Ifnε*$^{-/-}$ mice but not in WT mice (Figure 5A–C). In both the mid and proximal cervix of infected *Ifnε*$^{-/-}$ mice, ZIKV RNA was detected throughout the lamina propria and stroma. These findings suggest that IFNε may play a specific role in limiting the extent of viral spread in the FRT.

A role for IFNε in limiting the ascension of ZIKV toward the upper FRT was further supported by our observation that, while vaginal challenge caused mild genital erythema and inflammation of the CVT in both WT and *Ifnε*$^{-/-}$ mice (Figure S6), tissue edema in the uterus was observed only in *Ifnε*$^{-/-}$ mice but not in WT mice (Figure S7). Collectively, our findings highlight a specific function for IFNε in mediating protection against acute ZIKV infection via the vaginal route and suggest that IFNε may act to restrict viral spread beyond the lower CVT.

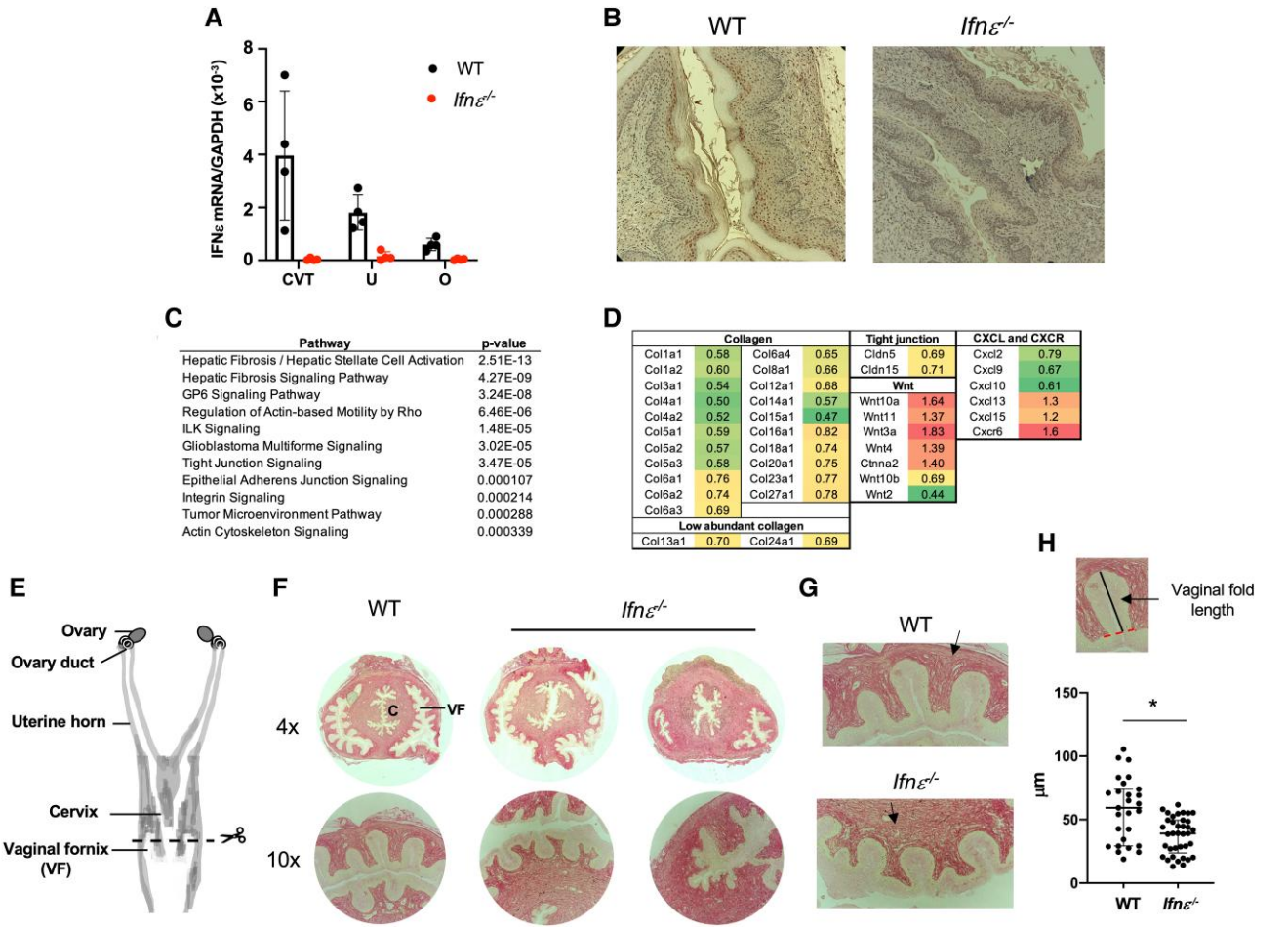

Fig. 3. *Ifnε*$^{-/-}$ mice exhibit an aberrant epithelial and tissue structure in the CVT. A) *Ifnε*$^{-/-}$ mice were generated using CRISPR/Cas9 technology. Knockdown of IFNε gene expression in the CVT, uteri (U), and ovaries (O) of *Ifnε*$^{-/-}$ mice was confirmed by RT-qPCR. B) IFNε protein expression in WT and *Ifnε*$^{-/-}$ mice was determined by immunohistochemistry (IHC). IFNε proteins (brown) were found in the vaginal tissue of WT mice but not in that of *Ifnε*$^{-/-}$ mice. C) and D) WT and *Ifnε*$^{-/-}$ mice were synchronized to the diestrus stage by Depo. Total RNAs from the CVT were collected on day 12 after injection. RNAseq analyses showing pathways (C) and genes (D) involved in epithelial integrity, tissue structure, and wound healing in the CVT of *Ifnε*$^{-/-}$ mice. E) A schematic diagram of a murine FRT. The site of sectioning for collagens and epithelial structure examination are indicated. F) Collagens in the cervix of WT and *Ifnε*$^{-/-}$ mice were stained with Picro Sirius Red. Cervical canal (C) and VF are indicated. G) Higher power views (20×) of vaginal epithelial folds and surrounding collagen structure. The black arrows show the difference in collagen organization. H) The length of vaginal epithelial folds in the mid regions of the vaginal epithelial fornix in WT and *Ifnε*$^{-/-}$ mice.

To determine whether the increased susceptibility of *Ifnε*$^{-/-}$ mice to ZIKV was due to impaired antiviral responses, we assessed the expression of IFN-stimulated genes (ISGs) in the CVT from infected mice. ISGs including genes encoding IFNα and 2′,5′-oligoadenylate synthetase were up-regulated to a comparable extent in the CVT of ZIKV-infected WT and *Ifnε*$^{-/-}$ mice (Figure S8). We also observed similar expression of *Ifnβ* transcripts in both cohorts, although total abundance at day 2 p.i was not significantly different from that at day 0. *Mx1* and *Isg15* were not induced. Taken together, these findings suggest that the increased susceptibility of IFNε mice to ZIKV is unlikely to be due to ISG expression during acute infection.

Recombinant mouse IFNε protein protects *Ifnar1*$^{-/-}$ mice against ZIKV infection

Recombinant IFNε proteins have been shown to protect mice against intravaginal HSV2 and *Chlamydia muridarum* infection (16). Therefore, we tested whether exogenous IFNε could protect mice against ZIKV infection. Vaginal administration of recombinant mouse IFNε protein protected *Ifnε*$^{-/-}$ mice against a subsequent intravaginal challenge with ZIKV (Figure 6A). Importantly, vaginal administration of recombinant IFNε, but not control linearized IFNε protein, was also sufficient to protect highly susceptible *Ifnar1*$^{-/-}$ mice from intravaginal ZIKV infection (Figure 6B and C), indicating that IFNε mediates protective effects through IFNAR1-independent mechanisms and is sufficient for protection even when signals from other type I IFNs are absent. IFNε-mediated host protection was specific to vaginal infection because the subcutaneous administration of recombinant IFNε did not protect *Ifnar1*$^{-/-}$ mice against subcutaneous ZIKV infection (Figure 6B). Additionally, IFNε proteins (4 μg) did not protect mice when administered to ZIKV-infected *Ifnar1*$^{-/-}$ mice on day 1 p.i. (Figure 6D), although a higher dose of IFNε proteins (8 μg) was able to suppress viral loads in the CVT of infected mice (Figure S9). In summary, our data demonstrate that exogenous IFNε is sufficient to provide FRT-specific and IFNAR1-independent protection against ZIKV infection when administered prior to infection, even in highly susceptible *Ifnar1*$^{-/-}$ mice.

Discussion

IFNε was previously reported to protect mice against HSV2 and *C. muridarum* infection in the FRT, but its mechanisms of action

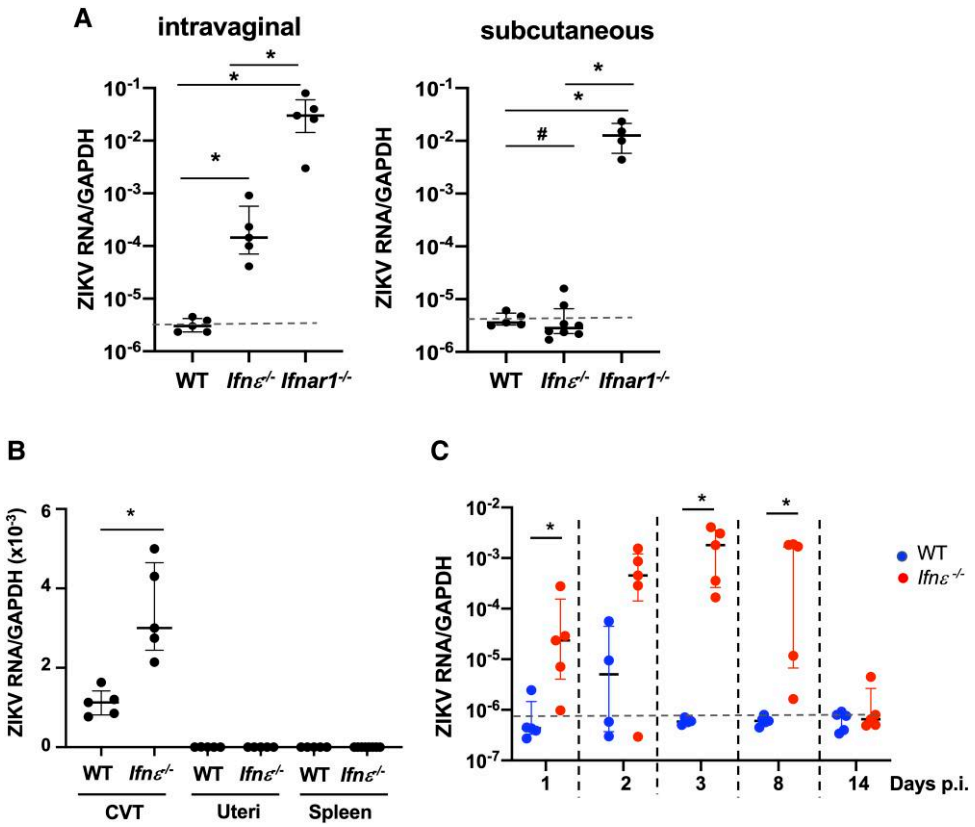

Fig. 4. *Ifnε*$^{-/-}$ mice exhibit increased susceptibility to intravaginal ZIKV infection. A) Depo-synchronized WT, *Ifnε*$^{-/-}$, and *Ifnar1*$^{-/-}$ mice were challenged with ZIKV PRVABC59 through an intravaginal or subcutaneous route. Zika RNA levels in the CVT were determined by RT-qPCR at day 3 p.i. The data represent five independent experiments. B) Depo-treated WT and *Ifnε*$^{-/-}$ mice were infected by ZIKV intravaginally. Total RNAs from the CVT, uteri, and spleen were harvested at day 3 p.i. Zika RNA levels were determined by RT-qPCR. The data represent three experiments. C) Depo-treated WT and *Ifnε*$^{-/-}$ mice were challenged with ZIKV intravaginally. Total RNAs of the CVT were prepared at different days p.i. ZIKV RNAs were quantified by RT-qPCR. The data represent three experiments. The dashed line indicates the background from uninfected mice. *$P < 0.05$; ns, not significant.

have remained incompletely understood (16). Our data suggest that IFNε may contribute to defense against microbial invasion in the FRT by ensuring maintenance of the epithelial barrier and tissue architecture in the CVT. Loss of IFNε disrupts this architecture and renders mice specifically susceptible to vaginal, but not subcutaneous, infection with ZIKV. In the context of vaginal infection, IFNε signaling not only limits the magnitude of ZIKV infection in the CVT but also restricts viral persistence and dissemination beyond the lower FRT. Critically, exogenous IFNε is sufficient to protect not only *Ifnε*$^{-/-}$ mice but also highly susceptible *Ifnar1*$^{-/-}$ mice from intravaginal ZIKV infection. Thus, IFNε is sufficient to protect against vaginal ZIKV infection even when signals from other type I IFNs are absent. Taken together, our data suggest that IFNε serves as a critical gatekeeper against ZIKV infection in the FRT, acting to prevent the ascension of the virus into deeper tissue compartments that are critical for reproduction.

Our findings have direct relevance to ZIKV infections transmitted through sexual contact as opposed to transmission via mosquitoes. Within this context, *Ifnε*$^{-/-}$ mice represent a useful model for studying ZIKV transmission and pathogenesis in the CVT. Because of the CVT-specific role of IFNε in host defense, it will be possible to study early and local aspects of ZIKV pathogenesis that can be difficult to study in *Ifnar1*$^{-/-}$ mice, which are highly immunodeficient and susceptible to uncontrolled viral replication and systemic dissemination (9, 33, 34).

A very recent report confirmed our findings of increased susceptibility of *Ifnε*$^{-/-}$ mice to intravaginal ZIKV infection (20). In this report, ZIKV was detected in vaginal wash but not in vaginal tissues in ZIKV-infected *Ifnε*$^{-/-}$ mice at day 5 p.i. However, ZIKV was detected in the uteri and ovaries (20). In our study, ZIKV was detected in the CVT but not in the tissues of the upper FRT at day 3 p.i. These discrepancies may be due to the differences existing in *Ifnε*$^{-/-}$ mouse lines, housing locations, duration of Depo treatment and ZIKV infection, and tissue preparation. A kinetic study on ZIKV signals from different regions of the FRT may provide insights into viral trafficking and clearance during the course of infection.

IFNε-mediated protection against viral infection in vitro is associated with the induction of ISGs (21, 22). However, ISG expression in the CVT was similar in ZIKV-infected *Ifnε*$^{-/-}$ and WT mice, suggesting that ISG induction may not be required for the protective functions of IFNε in this setting, at least at early time points. Instead, our data suggest a novel function for IFNε in maintaining barrier integrity in the CVT. We found that IFNε deficiency was associated with a dysregulated expression of genes implicated in wound healing and epithelial barrier function in the CVT of naïve *Ifnε*$^{-/-}$. These perturbations in gene expression were associated with abnormal collagen deposition and epithelial border structure in the vaginal tissue nearest to the cervix. Taken together with our finding of exacerbated viral spread in the CVT of *Ifnε*$^{-/-}$ mice, these data suggest that IFNε may restrict viral dissemination by maintaining proper barrier function in the FRT.

The mechanisms by which IFNε modulates collagen and epithelial homeostasis in the FRT are unknown. Various cytokines,

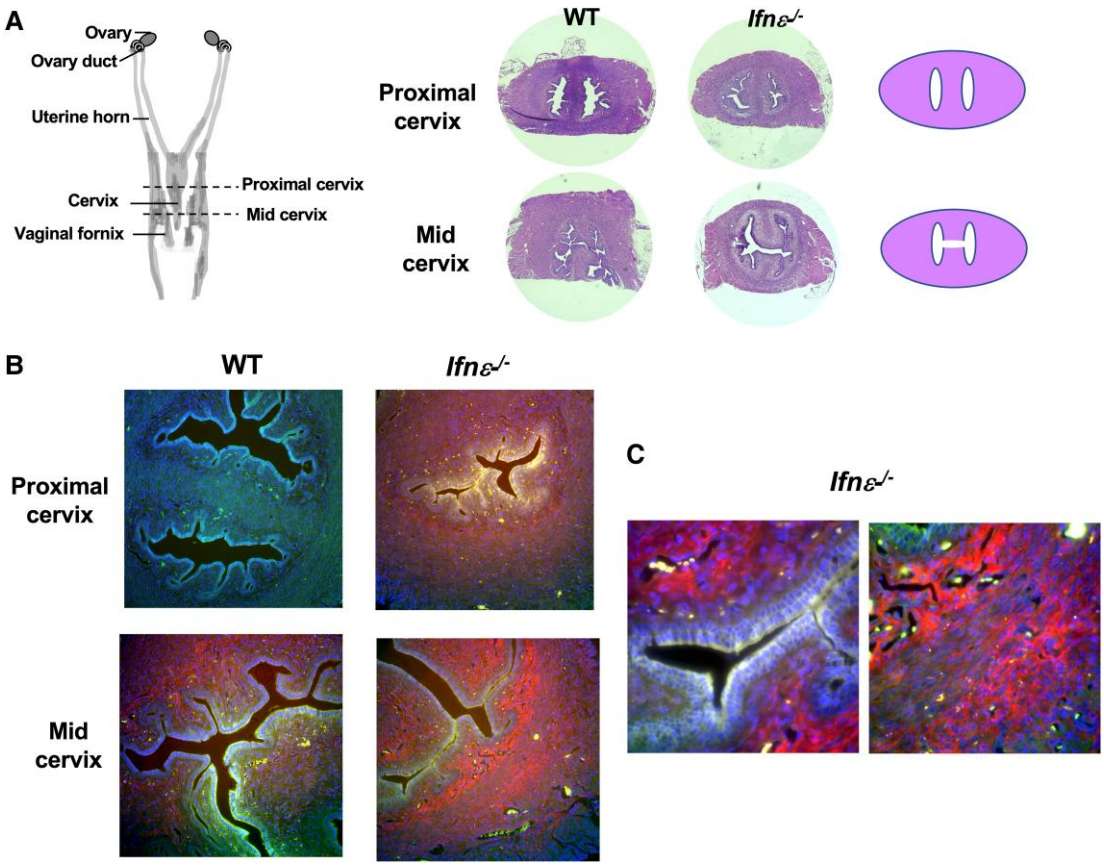

Fig. 5. Faster dissemination of ZIKV of *Ifnε*$^{-/-}$ mice. A) Serial sections of the CVT from the uterus fundus toward the distal cervix. H&E staining of the proximal and mid cervix of WT and of *Ifnε*$^{-/-}$ mice used for smFISH is shown. B). Adjacent sections to the H&E-stained sections were used for smFISH to detect ZIKV RNAs (red). Images at 20× are shown. Nuclei are in blue and autofluorescence is in green. Identical exposures were used for all images, including both WT and *Ifnε*$^{-/-}$ mice. C). Localization of ZIKA signals in *Ifnε*$^{-/-}$ mice (62×) in the lamina propria (left) and stroma (right).

including types I and II IFNs, transforming growth factor-β, and IL-1β, are known to modulate the synthesis of collagens required for the maintenance of tissue integrity at a steady state and during infection (36, 37). Other IFNs have been shown to regulate epithelial barrier function, including through effects on Wnt signaling (38–40). For example, IFNλ is constitutively expressed in gut and lung epithelial cells, where it regulates barrier integrity and mitigates inflammation-associated tissue damage during infection (41–44). We speculate that IFNε may exert similar functions in the epithelial and/or submucosal tissues of the FRT, and future studies on this topic are likely to deepen our understanding of the mechanisms by which IFNε protects against ZIKV and other sexually transmitted pathogens.

Prior studies reported high IFNε expression in epithelial cells and tissues in mouse and human FRT (16). Our data corroborate these findings, but further demonstrate IFNε expression by immune cells in the FRT of naïve mice and by human peripheral blood immune cells activated with specific viruses or TLR ligands. In particular, Sendai virus strongly induced, and HSV1 moderately induced, IFNε expression in human pDCs from all donors, whereas influenza virus and HIV did not. Likewise, TLR3 and TLR4 agonists, but not TLR2, TLR5, TLR7, or TLR9 agonists, induced a significant upregulation of IFNε expression in PBMCs. Our findings contrast with a prior work showing that TLR agonists do not induce IFNε in primary BMDMs, mouse embryonic fibroblasts, or a mouse macrophage cell line RAW264.7 (16). This same study reported that neither HSV2 nor *C. muridarum* infection drives increased IFNε expression in mouse uteri (16), whereas we found a significant increase in IFNε expression in CVT tissue in ZIKV-infected mice. These differences across studies suggest that IFNε expression is both cell-type- and stimulus-specific. Moreover, the ability of certain viruses, but not others, to induce IFNε expression may depend on which pathogen-sensing pathway is engaged. In support of this, HSV1 induces IFNα expression through the TLR9-MyD88 pathway (45), while the Sendai virus induces IFNα expression in pDCs via PKR-, TLR7/8-, and TLR9-independent pathways (46). The specific TLRs or pathogen-sensing pathways involved in Sendai- and HSV1-induced expression of IFNε in human pDCs or in ZIKV-induced mouse CVT remain to be determined.

Future studies are needed to determine whether IFNε produced by, or acting on, immune cells contributes to host protection in the FRT. However, IFNε has been shown to exert potent immunomodulatory effects on primary macrophages in vitro (21) to promote lymphocyte recruitment and protective CD8$^+$ T-cell responses in the lung during vaccinia virus infection (24), and to support natural killer cell recruitment in the FRT during chlamydial infection in mice (16). We speculate that IFNε signaling also regulates FRT immune responses to ZIKV infection. In support of this, our RNAseq data demonstrated altered chemokine and chemokine receptor expression in the CVT of naïve *Ifnε*$^{-/-}$ mice, highlighting a potential role for IFNε in regulating immune cell recruitment in the FRT even at a steady state.

Although IFNε was previously reported to signal through IFNAR1 and IFNAR2 in BMDMs (16), we show here that exogenous mouse IFNε proteins were sufficient to protect *Ifnar1*$^{-/-}$ mice against vaginal ZIKV infection, indicating that at least some antiviral activities

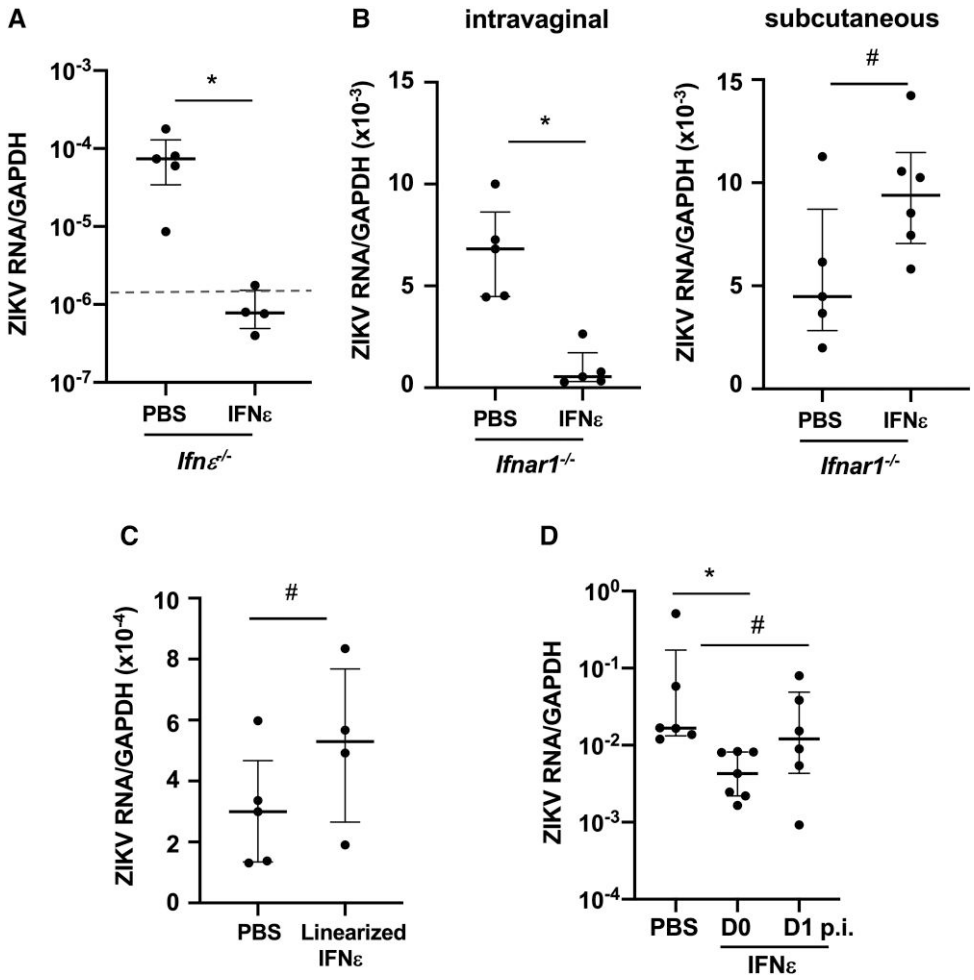

Fig. 6. Intravaginal administration of murine IFNε proteins protects mice against ZIKV infection. A) Depo-synchronized *Ifnε*$^{-/-}$ mice were treated with recombinant mIFNε proteins (4 μg) through an intravaginal route, followed by ZIKV infection 6 h later. ZIKV RNA levels in the CVT were determined by RT-qPCR at day 3 p.i. The dashed line indicates the background from uninfected control. B) Depo-synchronized *Ifnar1*$^{-/-}$ mice were treated with recombinant mIFNε proteins (4 μg) through an intravaginal or subcutaneous route, followed by Zika infection via the same route 6 h later. Zika RNA levels in the CVT and spleen were determined by RT-qPCR at day 3 p.i. C) Depo-synchronized *Ifnar1*$^{-/-}$ mice were treated with PBS or linearized mIFNε proteins (4 μg) intravaginally, followed by intravaginal ZIKV infection 6 h later. Viral RNA levels in the CVT were detected by RT-qPCR. D) Depo-synchronized *Ifnar1*$^{-/-}$ mice were treated with mIFNε proteins (4 μg) intravaginally 6 h before (D0) or 1 day after (D1) intravaginal ZIKV infection. Viral RNA levels in the CVT were detected by RT-qPCR. $^{*}P < 0.05$, $^{\#}P > 0.05$. The values of the background from uninfected Ifnar1$^{-/-}$ mice were $1–3 \times 10^{-6}$. The data represent three to four independent experiments.

of IFNε in this setting are IFNAR1-independent. Moreover, these activities are structure-dependent, as linearized IFNε protein failed to mediate protection. The mechanism by which recombinant IFNε proteins protect ZIKV infection remains to be determined. It is plausible that IFNε treatment strengthens the epithelial barrier, tissue structure, and innate immunity in the CVT.

In summary, we describe a novel role for IFNε in restricting viral replication and spread in the lower FRT during vaginal ZIKV infection in mice. We also demonstrate an FRT-specific role for IFNε in host defense against ZIKV infection, which is independent of IFNAR1 signaling, and we identify new cell type- and tissue–specific and stimulus-specific features of IFNε expression in the FRT and peripheral blood. Our findings offer insights into the potential use of IFNε to harness mucosal immunity for the prevention of STIs.

Materials and methods

Reagents

Histopaque-1077, fetal bovine serum (FBS), Roswell Park Memorial Institute (RPMI)-1640, Dulbecco's Modified Eagle Medium (DMEM), and phosphate-buffered saline (PBS) were procured from Sigma-Aldrich (St Louis, MO, USA). Human IFNα2α was purchased from PBL Assay Science (Piscataway, NJ, USA). Recombinant human IFN-λ1, IL-3, and IL-10 were purchased from PeproTech (Rocky Hill, NJ, USA). Human IL-2 was procured from R&D Systems (Minneapolis, MN, USA). Vero E6 cells were purchased from ATCC. ZIKV (PRVABC59 strain) was obtained from NIH Biodefense and Emerging Infections Research Resources Repository, NIAID, NIH. ZIKV was propagated in Vero E6 cells, and the virus titer was determined by plaque assays.

Murine IFNε proteins have three cysteine residues (C52, C162, and C174), which can contribute to different disulfide linkages. Recombinant mIFNε with a mutation of C174 to serine, a less conserved residue, had an improved capacity to induce ISGs (Figure S10) and was, therefore, used in these studies. The DNA constructs used to express recombinant murine IFNε and IFNε analog with the C174S replacement in *Escherichia coli* were synthesized and verified by Genescript (Piscataway, NJ, USA). For bacterial expression, a codon-optimized IFNε cDNA was cloned into pET28. Inclusion bodies of IFNε expressed in *E. coli* BL21, prepared

by Shenandoah Biotechnology, Inc (Warminister, PA, USA), were dissolved in 8 M GuHCl in the presence of DTT, purified by reversed-phase high-performance liquid chromatography, lyophilized, folded, and verified by electrospray ionization mass spectrometry, as described previously (21). Linear alkylated IFNε proteins were also prepared and verified by mass spectrometry, as described previously (21). The endotoxin level in IFNε was below 0.01 ng/mL as determined by Pierce LAL Chromogenic Endotoxin Quantitation Kit (Thermo Fisher Scientific).

Rabbit polyclonal antibodies against human or murine IFNε proteins were generated by using peptides derived from IFNε protein sequences (Lampire Biological Laboratories, Pipersville, PA, USA). The specificity of the antibodies was determined by performing western blot analysis. Preimmune sera were included as a control.

Human cell isolation and cervical tissue collection

PBMCs were isolated from the blood of healthy human donors obtained from the New York Blood Center by Histopaque-1077 gradient centrifugation. pDCs were isolated by negative selection from prepared PBMCs with the Human Plasmacytoid Dendritic Cell Isolation Kit-II from Miltenyi Biotec (Auburn, CA, USA) according to the manufacturer's instructions. The purity of enriched pDC ($CD123^+$blood dendritic cell antigen-2 $(BDCA\text{-}2)^+$, 90–99%) was determined by flow cytometry. Stimulation of pDCs with viruses or cytokines was performed as described previously (47). IFNα2 (1,000 IU/mL), IFN-λ1 (25 ng/mL), IL-3 (10 ng/mL), IL-10 (10 ng/mL), HSV1 strain 2931 at a multiplicity of infection of 1, influenza A virus PR/8/34 (4 hemagglutination U/mL), Sendai virus VR907 (16 hemagglutination U/mL), and (HIV-MN at 500 ng of p24/mL) were used to stimulate pDCs for 4 h.

Cervical tissues without gross pathology were obtained from women undergoing therapeutic hysterectomy. The tissues would be discarded otherwise. The study (Pro20140000108) was approved by Rutgers, New Jersey Medical School Institutional Review Board. No patient identifiers are associated with the tissues, and therefore, this study falls under Human Subject Research Exempt Category 4. Primary CECs were prepared as described previously (48).

Mice

The protocols for animal handling were approved by the Institutional Animal Care and Use Committee at Rutgers, New Jersey Medical School (PROTO999900732). Animals were housed in individually ventilated and filtered cages under positive pressure in an SPF facility. C57BL/6J (WT) and *Ifnar1*$^{-/-}$ mice on the same background were purchased from Jackson Laboratory (Bar Harbor, MA, USA). *Ifnε*$^{-/-}$ mice were generated on the C57BL/6J background by direct microinjection of CRISPR-Cas9 reagents into one-cell embryos. Founders 1 and 2 (Figure S3) were generated using 30 ng/μL Cas9 protein (PNABio), with 0.15 μM each of the crRNAs C110 CCTTGTACCACTCCAGTTCT and C112 ACTGAGAAGCAAGAGCCAAC along with 0.3 μM tracer RNA (Millipore-Sigma). Two founders were used to avoid the confounding effects of disrupted gene sequences from CRISPR-Cas9. Both founders exhibited the same phenotypes. Founder 1 had a 373-bp deletion removing the sequence from 49 bp upstream of the initiating methionine to codon 109, eliminating 2/3 of the IFNε coding sequence. Translation of the recombinant resulted in a C-terminal 54 AA peptide. Founder 1 also had a 12-bp deletion in the 3′UTR. Founder 2 had a 588-bp deletion removing the entirety of the IFNε coding sequence from 48 bp upstream of the initiating methionine to 22 bp downstream of the stop codon. A 107-bp segment containing the coding sequence of the first 32 AA was inserted at the deletion site in an inverted orientation. No open reading frames containing any part of IFNε were present. The primers used to genotype Founders 1 and 2 were IFNEE 5′-CTGGAATGGGAACCAGAAAACCTAAG-3′ and IFNEF 5′-CTAG CCATCTTAGAACACAGTTAACC-3′. The founders were confirmed by performing a Sanger sequencing of PCR fragments cloned into pCRTopo2.1 (Invitrogen). Transmitted alleles of disrupted *Ifnε* gene were confirmed in the F1 generation after crossing to C57BL/6J mice by Sanger sequencing.

To determine the effect of IFNε on host defense against ZIKVs, 8- to 12-week-old female mice were treated with 2 mg Depo subcutaneously. Synchronization at the diestrus stage was confirmed on days 12–14 after Depo treatment. Mice were infected with 8×10^3–1.5×10^4 PFU of ZIKV through an intravaginal or subcutaneous route. Clinical scores were assessed based on the following criteria: 0, no apparent signs of disease; 1, genital erythema; 2, moderate genital inflammation and swelling; 3, mucus, swelling, and redness with the presence of genital lesions; 4, severe genital lesions and/or hind limb paralysis as described by Fung et al. (16). Fat tissues associated with the FRT were removed physically and the specific regions of the FRT were harvested at indicated time points for RT-qPCR, smFISH, IHC, and collagen assays.

To determine IFNε expression in different cell types in the FRT, single-cell suspensions were generated as previously described (49). Briefly, the CVT, uteri, and ovaries were separated and minced with scissors and then digested with 1 mg/mL collagenase A (Sigma-Aldrich) and 0.1 mg/mL DNase (Roche) in RPMI-1640 (Gibco) with shaking at 250 rpm at 37°C twice for 15 min. Tissues were mechanically dissociated by passage through an 18- or 20-gauge needle after each shaking cycle. Cells were filtered through a 100-μm mesh and washed once with cold RPMI with 3% FBS (Fisher Scientific). Red blood cells (RBCs) were lysed with RBC lysis buffer (Tonbo Biosciences). EpCam+ epithelial cells, CD45+ immune cells, and EpCam-CD45- cells were sorted using fluorophore-conjugated antibodies against EpCam (clone G8.8; BioLegend, San Diego, CA, USA) or CD45 (clone 30-F11; eBiosciences) in a FACSAria II sorter (BD Biosciences, San Jose, CA, USA). Cell purity was >95%.

To prepare BMDMs from mice for testing murine IFNε activities, femurs were obtained from 8- to 12-week-old C57BL/6 mice. After euthanasia using CO_2, the femurs were dissected using scissors, cutting through the tibia below the knee joints as well as through the pelvic bone close to the hip joint. After removing the muscles connected to the bone, the femurs were rinsed in ice-cold 70% ethanol for 1 min, washed with PBS, and then both epiphyses were removed. The bones were flushed with a 10 mL syringe and a 27½-gauge needle with RPMI-1640 plus 10% FBS to extrude the bone marrow, which was then homogenized by pipetting. Bone marrow cells were then collected by centrifugation and incubated in a red blood cell lysis buffer at room temperature for 5 min. The cells (1×10^6) were cultured in RPMI-1640 with 10% FBS, gentamicin, amphotericin, and murine M-CSF at 40 ng/mL in a 10 cm dish for 5–6 days to obtain BMDMs.

Immunohistochemistry

The tissue sections of formalin-fixed, paraffin-embedded tissues were deparaffinized in xylene and rehydrated in a standard series of descending alcohol immersions. After antigen retrieval, the sections were stained with rabbit sera against murine IFNε (#24864) at a 1:400 dilution ratio and incubated at room

temperature for 50 min according to the immunohistochemistry protocol provided in the Dako Envision Kit (Aligent). The images were captured using an ECHO microscope.

Immunofluorescence microscopy

The tissue was mounted on slides, deparaffinized, and rehydrated. For antigen retrieval, the tissue was brought to 90°C in 10 mM sodium citrate (pH 6.0) for 10 min. The slides were allowed to cool and then placed in PBS for 10 min. The tissue was blocked in 5% FBS for 30 min and then washed three times in PBS, 0.05% Triton for 5 min/wash. The primary antibodies were diluted in SuperBlock (Thermo Fisher Scientific) and applied to the tissue overnight: rabbit sera against murine or human IFNε at a 1:200–500 dilution ratio, anti-E-cadherin murine mAb at 1:500 (cat# 61082; BD Biosciences), and anti-desmin murine mAb at 1:40–100 (clone DE-U-10, cat#SAB4200707, Sigma-Aldrich). The tissue was washed three times for 5 min/wash. The secondary Alexa Fluor *F(ab')*2 fragment antibody was diluted at 1:1000 in Superblock and applied to the tissue for 2 h. The tissues were counterstained with DAPI and mounted using a Vectashield mounting medium (Vector Labs, Burlingame, CA, USA). Images were acquired on a Nikon Eclipse Ti confocal microscope and analyzed by using NIS-Elements software.

Collagen staining

Collagen assays were performed using tissues from WT and *Ifnε*$^{-/-}$ mice from the same experiment, which were stained at the same time to reduce variability. The tissue sections were deparaffinized using xylene, hydrated through graded ethanol, and washed with distilled Mili-Q water. The tissue slides were then incubated with Picro Sirius Red Stain Kit (ab150681; Abcam, Cambridge, UK) for 60 min at room temperature according to the manufacturer's instructions. The slides were rinsed in acetic acid solution twice, dehydrated with 100% ethanol, and then mounted using glycerol. Images were captured on an ECHO Revolve Microscope.

Single-molecule fluorescence in situ hybridization

Serial 4 μm sections of formalin-fixed, paraffin-embedded tissue were prepared by Nationwide Histology (Missoula, MT, USA). smFISH for ZIKV RNA was performed following procedures described previously (50). A total of 48 3′-amino-labeled oligonucleotide probes for the NS1 region of ZIKV strain PRVABC59 were designed using the Stellaris Probe Designer with the highest stringency settings for the human host and then synthesized by LGC Biosearch Technologies. Probes were pooled, labeled with Cy5, and purified by HPLC (51). The sequences of the probes are listed in Table S2. The tissue slides were equilibrated in 2XSSC, 10% formamide in wash buffer and then hybridized in a 50 μL hybridization buffer containing 25 ng of pooled probes overnight at 37°C in a humid chamber. The coverslips were washed twice for 5 min with a wash buffer, equilibrated with 2XSSC supplemented with 0.4% glucose, and mounted using a deoxygenated mounting medium supplemented with DAPI (50). Images were acquired using a Zeiss Axiovert M200 microscope.

Real-time RT-qPCR

Mouse tissues were homogenized using soft-tissue homogenizing beads (VWR, Radnor, PA, USA). Total RNA was isolated using TRIzol (Life Technologies, Carlsbad, CA, USA). First-strand cDNA was synthesized by incubating 1,000 ng of total RNA with oligo(dT)$_{12–18}$ (25 μg/mL) or random primers (2.5 μM), and dNTPs (0.5 mM) at 65°C for 5 min, followed by quick-chilling on ice. Reverse transcription was performed at 42°C for 50 min and 70°C for 15 min using SuperScript III Reverse Transcriptase. The PCR contained cDNA equivalent to 50 ng of RNA input, 200 nM primer sets, and SYBR Green Master Mix (QIAGEN, Valencia, CA, USA) and was run on a StepOnePlus real-time PCR system (Life Technologies). The PCR conditions were 95°C denaturation for 10 min, 40 cycles of 95°C for 15 s, and 60°C for 60 s. The PCR products were quantified and normalized relative to the amount of GAPDH cDNA amplified in the same tube. The relative quantification of gene expression was calculated using the $2^{-\Delta\Delta Ct}$ (*Ct*, threshold cycle of real-time PCR) method according to the formula: $\Delta CT = Ct_{GAPDH} - Ct_{target}$, $\Delta\Delta Ct = \Delta Ct_{control} - \Delta C_{target}$. The primer sequences are listed in Table S3.

RNA-sequencing analysis

RNA sequencing from WT and *Ifnε*$^{-/-}$ mice was performed by Azenta using an Illumina sequencer. The analysis was performed in accordance with the nf-core RNA-sequencing guidelines (version 1.4.2). Briefly, the output reads were aligned to the GRCm38 genome using STAR (version 2.6.1d), followed by hit count generation using featureCounts (version 1.6.4) and StringTie (version 2.0). The read counts were normalized and compared for differential gene expression using DESeq2 (version 3.10) with significance at false discovery rate adjusted *P*-value <0.05. RNAseq data have been submitted to GEO (accession number: GSE228359). To identify the pathways/networks and biological functions perturbed in *Ifnε*$^{-/-}$ mice compared with WT mice, the significant differentially expressed genes were analyzed using Ingenuity Pathway Analysis (INGENUITY, QIAGEN, Redwood City, CA, USA) as described in (52). Fisher's exact test was used to calculate the *P*-values used to rank the networks of significantly differentially expressed genes (SDEG); $P < 0.05$ was considered statistically significant.

Statistical analysis

Statistical comparisons were performed using the Mann–Whitney *U* test or one-way ANOVA with Tukey's post hoc tests; $P < 0.05$ was considered significant.

Acknowledgments

The authors thank Amy Rosenfeld and Vincent Racaniello for the technical support on the Zika viral infection assay, Pierre Lespinasse and Debra Heller for their support on acquiring human cervical tissues, Pam De Lacy and her team at Shenandoah Biotechnology, Inc for the production of IFNε proteins in *E. coli*, Peter Romanienko at Rutgers, genomic editing core facility for generating *Ifnε*$^{-/-}$ mice, Heather Marlatt at Nationwide Histology for the preparation of tissue sections, and Eric Milner for editing the manuscript.

Supplementary Material

Supplementary material is available at *PNAS Nexus* online.

Funding

This work was supported by National Instiute of Health grants R01AI36948 to T.L.C., and R01 CA227291 to S.T.

Preprints

The manuscript was posted on a preprint: https://www.biorxiv.org/content/10.1101/2023.04.06.535968v1.

Data Availability

All data required for the main findings of this manuscript are included in the article and Supplementary Materials. The Accession number of RNAseq data from GEO is GSE228359.

References

1 Pavlidis I, *et al.* 2020. Cervical epithelial damage promotes *Ureaplasma parvum* ascending infection, intrauterine inflammation and preterm birth induction in mice. *Nat Commun*. 11:199.
2 Lacroix G, Gouyer V, Gottrand F, Desseyn JL. 2020. The cervicovaginal mucus barrier. *Int J Mol Sci*. 21:8266.
3 Lozenski K, Ownbey R, Wigdahl B, Kish-Catalone T, Krebs FC. 2012. Decreased cervical epithelial sensitivity to nonoxynol-9 (N-9) after four daily applications in a murine model of topical vaginal microbicide safety. *BMC Pharmacol Toxicol*. 13:9.
4 Catalone BJ, *et al.* 2004. Mouse model of cervicovaginal toxicity and inflammation for preclinical evaluation of topical vaginal microbicides. *Antimicrob Agents Chemother*. 48:1837–1847.
5 Fichorova RN, Desai PJ, Gibson FC 3rd, Genco CA. 2001. Distinct proinflammatory host responses to *Neisseria gonorrhoeae* infection in immortalized human cervical and vaginal epithelial cells. *Infect Immun*. 69:5840–5848.
6 Van Damme L, *et al.* 2002. Effectiveness of COL-1492, a nonoxynol-9 vaginal gel, on HIV-1 transmission in female sex workers: a randomised controlled trial. *Lancet*. 360:971–977.
7 Pierson TC, Diamond MS. 2018. The emergence of Zika virus and its new clinical syndromes. *Nature*. 560:573–581.
8 Lopez CA, Dulson SJ, Lazear HM. 2022. Zika virus replicates in the vagina of mice with intact interferon signaling. *J Virol*. 96: e0121922.
9 Yockey LJ, *et al.* 2016. Vaginal exposure to Zika virus during pregnancy leads to fetal brain infection. *Cell*. 166:1247–1256.e4.
10 Musso D, Gubler DJ. 2016. Zika virus. *Clin Microbiol Rev*. 29: 487–524.
11 Counotte MJ, *et al.* 2018. Sexual transmission of Zika virus and other flaviviruses: a living systematic review. *PLoS Med*. 15: e1002611.
12 Chibueze EC, *et al.* 2017. Zika virus infection in pregnancy: a systematic review of disease course and complications. *Reprod Health*. 14:28.
13 Rodríguez Y, *et al.* 2018. Guillain-Barré syndrome, transverse myelitis and infectious diseases. *Cell Mol Immunol*. 15:547–562.
14 Acosta-Ampudia Y, *et al.* 2018. Autoimmune neurological conditions associated with Zika virus infection. *Front Mol Neurosci*. 11: 116.
15 Hardy MP, Owczarek CM, Jermiin LS, Ejdeback M, Hertzog PJ. 2004. Characterization of the type I interferon locus and identification of novel genes. *Genomics*. 84:331–345.
16 Fung KY, *et al.* 2013. Interferon-epsilon protects the female reproductive tract from viral and bacterial infection. *Science*. 339: 1088–1092.
17 Xi Y, Day SL, Jackson RJ, Ranasinghe C. 2012. Role of novel type I interferon epsilon in viral infection and mucosal immunity. *Mucosal Immunol*. 5:610–622.
18 Eid SG, Mangan NE, Hertzog PJ, Mak J. 2015. Blocking HIV-1 transmission in the female reproductive tract: from microbicide development to exploring local antiviral responses. *Clin Transl Immunol*. 4:e43.
19 Abdulhaqq SA, *et al.* 2016. HIV-1-negative female sex workers sustain high cervical IFNvarepsilon, low immune activation, and low expression of HIV-1-required host genes. *Mucosal Immunol*. 9:1027–1038.
20 Coldbeck-Shackley RC, *et al.* 2023. Constitutive expression and distinct properties of IFN-epsilon protect the female reproductive tract from Zika virus infection. *PLoS Pathog*. 19:e1010843.
21 Tasker C, *et al.* 2016. IFN-epsilon protects primary macrophages against HIV infection. *JCI Insight*. 1:e88255.
22 Zhao FR, Wang W, Zheng Q, Zhang YG, Chen J. 2022. The regulation of antiviral activity of interferon epsilon. *Front Microbiol*. 13: 1006481.
23 Peng FW, *et al.* 2007. Purification of recombinant human interferon-epsilon and oligonucleotide microarray analysis of interferon-epsilon-regulated genes. *Protein Expr Purif*. 53:356–362.
24 Day SL, Ramshaw IA, Ramsay AJ, Ranasinghe C. 2008. Differential effects of the type I interferons alpha4, beta, and epsilon on antiviral activity and vaccine efficacy. *J Immunol*. 180: 7158–7166.
25 Mungin JW Jr, Chen X, Liu B. 2022. Interferon epsilon signaling confers attenuated Zika replication in human vaginal epithelial cells. *Pathogens*. 11:853.
26 Matsumiya T, Prescott SM, Stafforini DM. 2007. IFN-epsilon mediates TNF-alpha-induced STAT1 phosphorylation and induction of retinoic acid-inducible gene-I in human cervical cancer cells. *J Immunol*. 179:4542–4549.
27 Pinto D, Gregorieff A, Begthel H, Clevers H. 2003. Canonical Wnt signals are essential for homeostasis of the intestinal epithelium. *Genes Dev*. 17:1709–1713.
28 Ali A, *et al.* 2020. Cell lineage tracing identifies hormone-regulated and Wnt-responsive vaginal epithelial stem cells. *Cell Rep*. 30:1463–1477.e7.
29 Lam AP, Gottardi CJ. 2011. β-catenin signaling: a novel mediator of fibrosis and potential therapeutic target. *Curr Opin Rheumatol*. 23:562–567.
30 Astudillo P. 2020. Extracellular matrix stiffness and Wnt/β-catenin signaling in physiology and disease. *Biochem Soc Trans*. 48:1187–1198.
31 Wehner D, *et al.* 2017. Wnt signaling controls pro-regenerative Collagen XII in functional spinal cord regeneration in zebrafish. *Nat Commun*. 8:126.
32 Liu J, *et al.* 2020. Wnt4 negatively regulates the TGF-β1-induced human dermal fibroblast-to-myofibroblast transition via targeting Smad3 and ERK. *Cell Tissue Res*. 379:537–548.
33 Morrison TE, Diamond MS. 2017. Animal models of Zika virus infection, pathogenesis, and immunity. *J Virol*. 91:e00009-17.
34 Lazear HM, *et al.* 2016. A mouse model of Zika virus pathogenesis. *Cell Host Microbe*. 19:720–730.
35 Khan S, *et al.* 2019. Low expression of RNA sensors impacts Zika virus infection in the lower female reproductive tract. *Nat Commun*. 10:4344.
36 van der Zee E, Everts V, Beertsen W. 1997. Cytokines modulate routes of collagen breakdown. Review with special emphasis on mechanisms of collagen degradation in the periodontium and the burst hypothesis of periodontal disease progression. *J Clin Periodontol*. 24:297–305.
37 Granstein RD, Flotte TJ, Amento EP. 1990. Interferons and collagen production. *J Invest Dermatol*. 95:S75–S80.
38 Tschurtschenthaler M, *et al.* 2014. Type I interferon signalling in the intestinal epithelium affects Paneth cells, microbial ecology and epithelial regeneration. *Gut*. 63:1921–1931.

39 Katlinskaya YV, *et al.* 2016. Type I interferons control proliferation and function of the intestinal epithelium. *Mol Cell Biol*. 36: 1124–1135.

40 Kotredes KP, Thomas B, Gamero AM. 2017. The protective role of type I interferons in the gastrointestinal tract. *Front Immunol*. 8:410.

41 Lazear HM, Nice TJ, Diamond MS. 2015. Interferon-λ: immune functions at barrier surfaces and beyond. *Immunity*. 43:15–28.

42 Lazear HM, Schoggins JW, Diamond MS. 2019. Shared and distinct functions of type I and type III interferons. *Immunity*. 50:907–923.

43 Stanifer ML, Guo C, Doldan P, Boulant S. 2020. Importance of type I and III interferons at respiratory and intestinal barrier surfaces. *Front Immunol*. 11:608645.

44 Odendall C, Voak AA, Kagan JC. 2017. Type III IFNs are commonly induced by bacteria-sensing TLRs and reinforce epithelial barriers during infection. *J Immunol*. 199:3270–3279.

45 Krug A, *et al.* 2004. Herpes simplex virus type 1 activates murine natural interferon-producing cells through toll-like receptor 9. *Blood*. 103:1433–1437.

46 Hornung V, *et al.* 2004. Replication-dependent potent IFN-α induction in human plasmacytoid dendritic cells by a single-stranded RNA virus. *J Immunol*. 173:5935–5943.

47 Deb P, Dai J, Singh S, Kalyoussef E, Fitzgerald-Bocarsly P. 2020. Triggering of the cGAS–STING pathway in human plasmacytoid dendritic cells inhibits TLR9-mediated IFN production. *J Immunol*. 205:223–236.

48 Couret J, *et al.* 2017. Differential regulation of IFNalpha, IFNbeta and IFNepsilon gene expression in human cervical epithelial cells. *Cell Biosci*. 7:57.

49 Valero-Pacheco N, *et al.* 2022. Maternal IL-33 critically regulates tissue remodeling and type 2 immune responses in the uterus during early pregnancy in mice. *Proc Natl Acad Sci U S A*. 119: e2123267119.

50 Raj A, van den Bogaard P, Rifkin SA, van Oudenaarden A, Tyagi S. 2008. Imaging individual mRNA molecules using multiple singly labeled probes. *Nat Methods*. 5:877–879.

51 Raj A, Tyagi S. 2010. Detection of individual endogenous RNA transcripts in situ using multiple singly labeled probes. *Methods Enzymol*. 472:365–386.

52 Subbian S, *et al.* 2013. Early innate immunity determines outcome of *Mycobacterium tuberculosis* pulmonary infection in rabbits. *Cell Commun Signal*. 11:60.